Geoenvironmental Disasters

RESEARCH

Open Access

Using VIIRS nightlights to estimate the impact of the 2015 Nepal earthquakes

Thomas Tveit[1*], Emmanuel Skoufias[2] and Eric Strobl[1]

Abstract

We use Visible Infrared Imaging Radiometer Suite (VIIRS) nightlight data to model the impact of the 2015 Nepal earthquakes. More specifically, the data—showing nightlight emissions—are used to examine the extent to which there is a difference in nightlight intensity between cells damaged in the earthquake versus undamaged cells based on (1) mean comparisons; and (2) fixed effect regression models akin to the double difference method. The analysis is carried out for the entire country as well as smaller regions in and around the Central area and Kathmandu, which were the hardest hit areas. Overall, the regressions find a significant and negative effect from the initial shock, followed by a positive net effect from aid and relief efforts, which is consistent with what one would expect to find. However, the mean analysis results are inconclusive and there is substantial noise in the nightlight measurements due to how the values are produced and persistent cloud cover over Nepal.

Keywords: Earthquakes, Night-time lights (NTL), VIIRS, Remote sensing, Econometrics

Introduction

The Gorkha earthquake that struck Nepal on 25 April 2015 is one of the biggest natural hazards of the last decade. The widespread damages totalled USD 10 billion in monetary damages, leaving 8857 dead, 22,304 injured and tens of thousands homeless. In addition to the main earthquake, several significant aftershocks also occurred, causing additional damages and deaths. Following any natural hazard of this scale, it is important to quickly and accurately identify the areas which are most in need of aid and where one can expect the highest damages, both in terms of casualties and monetary losses. The two are often correlated as the level of human activity usually coincides with economic output. Often, the identification of damages are done by on the ground observations or by manually examining images taken from air or from space, but over the last two decades a growing body of literature has focused on using remotely sensed data and automated algorithms to analyze and detect changes caused by natural hazards, see for example Elliott et al. (2015), Klomp (2016), Skoufias et al. (2017), Nguyen and Noy (2019) or Gao et al. (2020).

The aim of this paper is to build upon this literature by showcasing how high-resolution nightlight and population data can be used to quantify highly localized changes in economic activity as proxied by monthly nightlight data. By using population data as a secondary layer, we seek to avoid several known issues with the nightlight value measurements, such as blooming, airglow contamination and rural area values being more poorly correlated with economic activity. In addition, while existing articles have focused on identifying affected areas immediately after impact, this paper uses mean analysis and fixed effects regressions to quantify the initial impact and temporal effect over the 12 months ex-post. This is similar to Gao et al. (2020), but whereas they examined purely based on nightlight change, we use objectively measured earthquake data to identify nightlight cells that were impacted by the earthquake and compared these with cells that experienced no damage.

The methodology of this paper is the same as used in Skoufias et al. (2021), where the authors found that VIIRS

*Correspondence: Thomas.tveit@vwi.unibe.ch
[1] Department of Economics, University of Bern, Schanzeneckstrasse 1, 3001 Bern, Switzerland
Full list of author information is available at the end of the article

nightlight data provided limited results when analyzing larger countries and numerous natural hazards. In this paper, we use the same method, but across a smaller area and on a more damaging hazard, making it arguably an ideal setting for performing such an analysis. In short, we use contour maps from the United States Geological Survey (USGS) to identify damaged areas and model the local damage at a cell level from vulnerability curves provided by International and Regional Development (2001). The damage data is then geomapped alongside the VIIRS and population data, which act as a proxy for the economic activity and hence the asset exposure. Finally, the combined data is used to identify and quantify what impact the damage has on nightlight values in two different analysis. The first is a mean comparison between damaged and non-damaged nightlight cells and the other is a fixed effect regression.

The nightlights data used in literature has primarily been from two sources: the Defense Meteorological Satellite Program (DMSP) and the VIIRS. The former is discontinued and consists of annual data from 1992 through 2013 with the data released being grid cells at 30 arc-second resolution (approximately 1 km by 1 km at equator) where each cell has a normalized digital number (DN) value from 0 to 63. The VIIRS data is more recent (April 2012 and onwards), has improved spatial and temporal detail with monthly releases at a grid cell resolution of 15 arc-seconds and the DN values have no upper bound. However, despite the advantages of the VIIRS data, it does have some limitations. Firstly, it is much more volatile than the DMSP data and due to stray light correction it can contain negative light values. Furthermore, some months have no measurements because of cloud cover. Despite these shortcomings, the VIIRS data values does show some correlation with local GDP (Zhao et al. 2017) and we will use it as a proxy for economic activity in this article.

To improve upon the VIIRS data and attempt to decrease the volatility, we will use a settlement layer as a secondary layer to better identify areas with human activity. Using secondary data sources to increase the likelihood of correctly identifying human settlements have previously been used for poverty (Jean et al. 2016) and urban extent (Baragwanath et al. 2019). The data used is from Worldpop (2017), which utilizes satellite images and census data to construct a high-resolution layer of human settlement patterns. The inclusion of the additional data is used to exclude non-populated cells and to better distinguish rural and urban areas.

Finally, to identify and model local damage, we construct a damage index based on ShakeMaps from the USGS. The damage estimates are then combined with the economic activity proxy and two types of analysis are performed on the combined data. First, a simple mean comparison is performed where we compare the nightlight values between affected and non-affected cells for the 12 months before and after the earthquake. Secondly, we run a fixed effect regression model to identify and quantifyimpact over the first 12 months ex-post. Both analysis are performed on a national nightlight set as well as sets on smaller regions that were more severely impacted by the earthquakes.

The mean analysis results are not significant, potentially due to the general volatility and measurement errors in the data. However, it could also be caused by an influx of aid and recovery to all areas of Nepal and not just the ones experiencing the most damage, i.e. if aid is not well targeted one would experience the same pattern across all cells. When performing a pre-post analysis of the mean results, we do find that there is a significant difference in the trajectories of the two groups. To further support this, the fixed effects regressions did yield significant results, with an initial negative and significant shock in the month of the disaster, followed by a statistically significant increase in light for 4–6 months, before tapering off and becoming insignificant. The first negative shock followed by a positive effect is consistent with what one could expect from a large-scale disaster, where at first infrastructure is damaged and necessary aid is not present, followed by an influx of aid and relief efforts over the coming months. Following this phase, one would expect a decrease in nighlight values as the initial relief efforts are discontinued. Additionally, after 12 months one can potentially expect the VIIRS values to reflect a "new" normal and any significant effects found after that are unlikely to be directly related to the earthquake.. However, the regression results include an unexpected and sudden positive spike 12 months after the earthquakes. The cause for this is unknown and the most likely explanation is that it is caused by noise in the measurements. The regressions were run with several different specifications as robustness checks, but the main results remained unchanged.

The remainder of the paper starts with an overview of Nepal, the earthquakes and the base data, followed by a general methodology overview, the analysis results and finally a conclusion.

Materials and methods

Nepal and the 2015 earthquakes

Nepal is a mountainous country bordering India to the south, west and east and Tibet (China) to the north. It is a small country at roughly 147,000 square kilometers and has a population of approximately 29 million people. Its nominal GDP in 2019 is USD30.6 billion. On a per

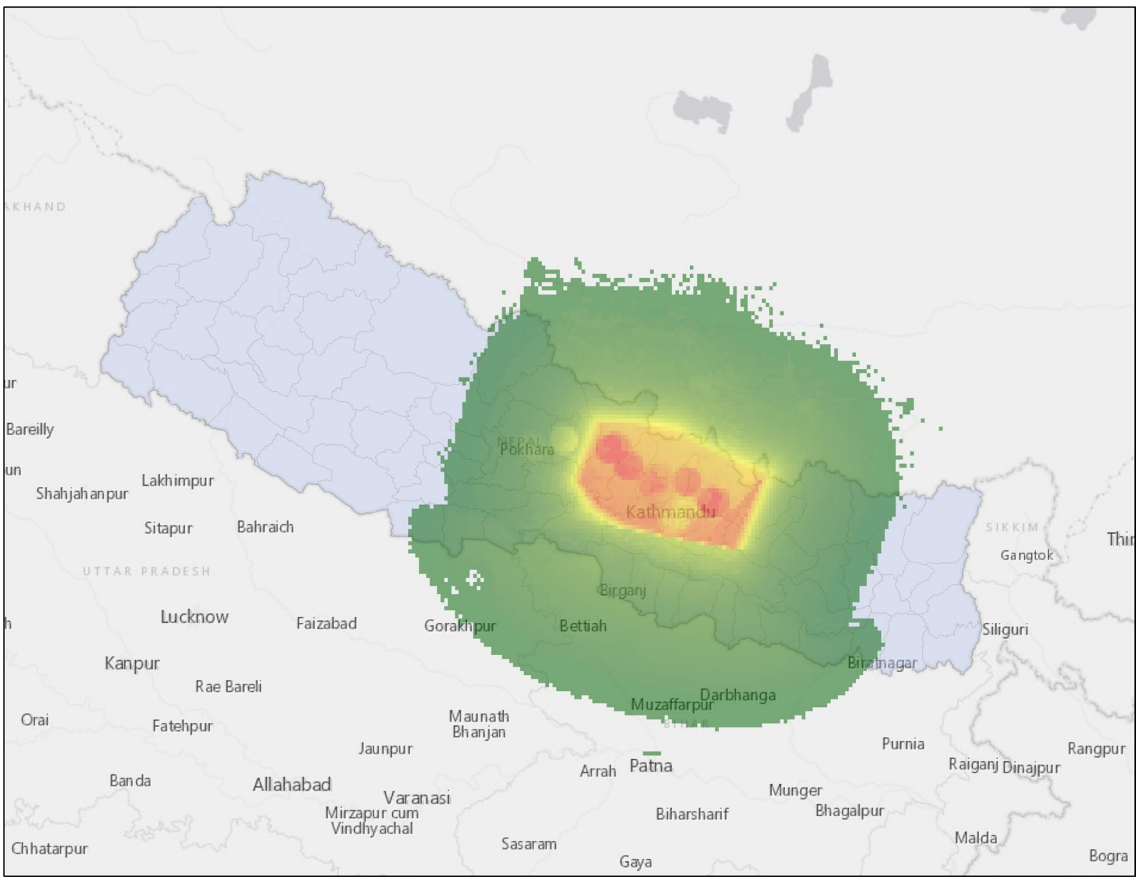

Fig. 1 Nepal and the Gorkha earthquake. The underlying blue colour shows Nepal, whereas the green to red outlines the extent and intensity of the earthquake, with red being the most impacted areas. *Source*: USGS Shakemap and ArcGIS Basemap

capita purchasing power adjusted basis, Nepal ranks at the 162nd position globally per the World Bank.

In addition, Nepal is prone to disasters due to a combination of the vulnerability of the building environment and the population, its geographical location, topography and climate. Nepal is frequently affected by different types of natural hazards such as landslides, floods and avalanches, stemming from the topography and the climate. Due to lack of irrigation, drought and fire are other frequent natural hazards. Finally, Nepal is situated alongside a major east–west tectonic boundary plate where earthquakes are frequent. INFORM earthquake exposure rank them at an 9.9 out of 10 (INFORM 2019).

In 2015, Nepal suffered two major earthquakes. The first—and largest—earthquake struck on 25 April 2015 and is often referred to as the Gorkha Earthquake. Figure 1 shows the magnitude and size of the 7.8 MW earthquake relative to Nepal and the epicenter in the Gorkha District. According to the UN office for Disaster Risk Reduction the total damages added up to USD 10 billion—approximately one third of the total GDP—with 8857 mortalities and 22,304 injured. In addition, tens of thousands were made homeless. Some damages were also due to landslides caused by the earthquake as seen in Xu et al. (2017). In this paper, we will treat all damages as earthquake damages as the effect on nightlights will be the same and the cause of the damage is the earthquake. Furthermore, to disentangle the two at a regional or national scale would require significant manual labor.

In the wake of the Gorkha earthquake there were several aftershocks, with the largest one being a magnitude 7.3 MW occurring on 12 May 2015 to the east of Kathmandu in the districts of Dolakha and Sindhupalchowk. There were 153 dead and 3275 injured following this earthquake.

The data used to identify the damaged areas and model the damage are from contour maps generated by seismological ground stations (International and Regional Development 2001; Agency 2006; De Groeve et al. 2008). These contour maps—ShakeMaps from USGS—are used as a basis for localized impact and they provide several key parameters such as peak ground acceleration (PGA),

peak ground velocity (PGV) and modified Mercalli intensity (MMI). The maps use data from seismic stations and combine this with information on ground conditions and earthquake depth to interpolate and construct a grid of points spaced 0.0167 degrees apart.

Population layer

To properly capture economic activity through nightlights it is important to correctly identify areas with people, hence avoiding stray lights or other sources of light that are not connected to human activity. One method is to use a human settlement layer as a secondary data set, such as in Corbane et al. (2016). One assumes that the settlement layer provides a better static map of the spatial distribution of people and then the nightlight data provide a temporal and spatial overview of how the economic activity is distributed within the populace.

In this paper, we use the Worldpop datasets to identify settlement areas in Nepal (Worldpop 2017). These datasets have a spatial gridcell resolution of approximately 100 m at the equator and estimate the number of persons per square for the years 2010, 2011 (based on census data), 2015 and 2020. This article uses only the 2015 estimates as these are from the same year as the earthquakes. Worldpop constructed the population files by using national totals and then adjust these to match UN population estimates. The adjustment is done by a Random Forest model, which generates a weighted population density layer and then this layer is used as a basis to place the population according to the assumed real geographical distribution.

In addition to identifying economic activity, the settlement layers will be used to designate a cell as rural and urban based upon population density.

VIIRS

To find and identify areas with economic activity and their exposure to natural hazards, satellite images of nighttime lights will be used as a proxy. Since natural hazards are highly localized, one would prefer high-resolution spatially disaggregated economic data, although nightlights have been used successfully to model local economic activity (Henderson et al. 2012; Gillespie et al. 2014; Hodler and Raschky 2014; Michalopoulos and Papaioannou 2014). These articles use the annual DMSP data with 30-arc second grids, whereas more recent papers have also utilized the VIIRS Day/Night Band (DNB) provided by The Earth Observations Group (EOG) at NOAA/NCEI, see for example Chen and Nordhaus (2015), Zhao et al. (2017, 2018) or (2020). The latter data set provides monthly data from April 2012 till present, whereas DMSP contains nightlight data for the years 1992 through 2013, making DMSP unusable for studying the Nepal earthquake. Recently, Sahoo et al. (2020) have utilized machine learning methods to intercalibrate between the two data sets and construct a longer annual data set. However, an increase in the length of the temporal dimension at the cost of temporal detail is not beneficial in this study. Additionally, data that is prior to 2012 is unlikely to impact on the 2016 estimated effects.

The use of VIIRS in economic analysis was done early in its lifetime by Chen and Nordhaus (2015), where they found promising results for VIIRS as an economic and population indicator, also when compared to the DMSP product. However, the same authors found that VIIRS was not useful in growth predictions and that the association between economic activity and light values were dependent upon the chosen area size, with state level analysis performing worse than metropolitan area level analysis (Chen and Nordhaus 2019). They hypothesized that this was in part due to the economic activity type in metropolitan areas and that they are more likely to be related to electric light. In a more recent working paper, Gibson et al. (2019) also find that VIIRS performs poorly in rural, low-density areas in Indonesia, while it performs well and much better than DMSP data in urban areas. The VIIRS products have also seen use in the natural disaster literature with Zhao et al. (2018) using the underlying NPP-VIIRS DNB Daily Data to analyze selected natural disasters, including the Gorkha earthquake. They found that the images could be used in damage detection and for identifying power outages, but that the analysis was limited by cloud coverage. This article will not use the daily data because of computational limitations when focusing on much longer temporal and spatial effects.

The VIIRS data provide two variables: the average monthly light radiance from DNB and the number of cloud free days. Some months will have no cloud free days, meaning that no radiance value is provided. This is accounted for by calculating an interpolated value from the values of the month prior and after.[1] In addition, a known problem for low light value cells is that one often finds negative light values due to airglow contamination (Uprety et al. 2019). Optimally, one would want to correct for this and identify the real underlying value and decrease the volatility exhibited. Recently, two published articles (one about the Gorkha earthquake) have explored methodologies for correcting the measurements through trend decompositions (Gao et al. 2020; Zhao et al. 2020). However, lacking any established methodology, we experimented by using simple threshold testing to identify how it would affect the analysis.

[1] Using the value of the month of the previous year was also explored, but the overall value mean change was less than 0.01 and there were only 1 cell that was affected by the earthquake that had no radiance value.

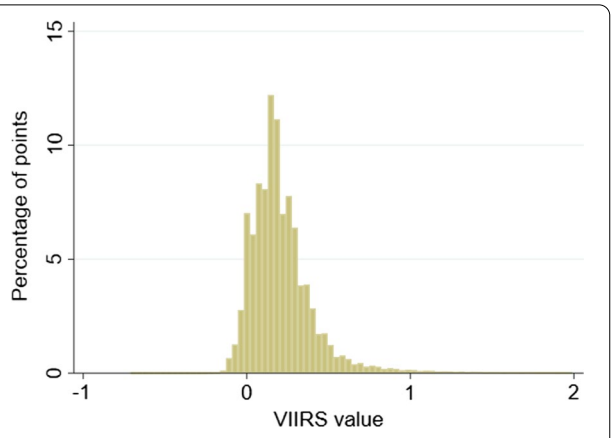

Fig. 2 VIIRS value distribution for VIIRS values below 2

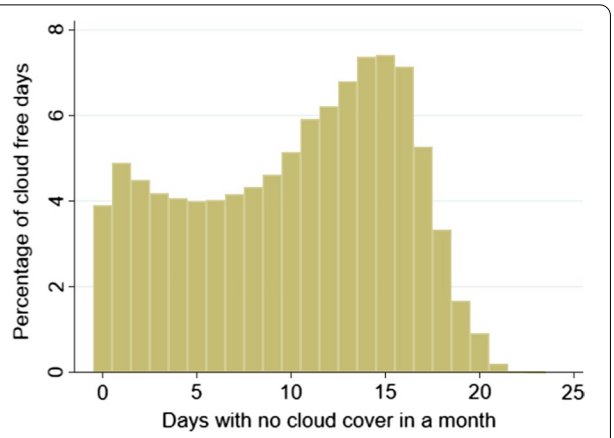

Fig. 3 Days with no cloud cover in a month across all months. The X-axis shows how many days per month that were cloud free, i.e. that had a light value measurement. The Y-axis shows the distribution of number of cloud free days per month. Adding up all columns equal 1

Figure 2 show the distribution of VIIRS values below 2 for all populated areas and the number of cloud free days per month.[2] It identifies significant clustering between the values 0 and 0.5, containing more than 85 percent of the total observations. Furthermore, more than 5% of the total have a negative value. Analyzing the range from negative to 0.3, one finds that 75% of all points fall within this range, implying that a large proportion of our observations have negative or very small values. These are only points that have been identified as being populated,[3] meaning that they should be relatively free of disturbance from non-human sources.

Even when limiting the observations to cells with population in excess of 50 (approximately 30% of populated cells), the distribution stays similar with 98 percent of light values being below 2, 95% below 1, 58% below 0.3 and 3% being negative. This distribution pattern is consistent independently of which population threshold is chosen. When looking at population numbers above 1000 (less than 0.5% of the total) 9% of the points still have nightlight values below 0.3 albeit less than 0.01% of points have values below 0, implying that VIIRS is potentially only useful for urbanized areas with a high population density.

Figure 3 provides an overview of the distribution of cloud free days, with each pillar representing the percentage of observations for all months depending on the number of cloud free observations. From this, we find that no months have more than 23 cloud free days and only 1% of months have 20 or more observations. At the same time, almost 10% of the monthly observations had 0 or 1 cloud free days, with 4% of the sample having no observations. The months with no cloud free days were included either through interpolation or by using the prior year's value. The median and mean are 10, and more than 12% of months had one or less cloud free days. Hence, the monthly nightlight values are calculated based on a rather small subsample of days per month. However, for a natural hazard which is not correlated with the weather, such as earthquakes, this is unlikely to bias the results. In the data, April 2015 had a maximum number of cloud free days at just 16, and a mean and median at 9, whereas May had a maximum number of cloud free days at 19 with a mean of 11 and median of 12. Overall, the year of 2015 was quite similar to the total sample, with a max of 20, mean of 9 and median of 10. However, the relatively low number of cloud free days for April could potentially impact the analysis. Another factor that could bias the results would be the monsoon season months from June through August, this will be commented upon in the discussion section.

General empirical strategy

The approach chosen is the same as in Skoufias et al. (2021), where the authors constructed damage indices that were combined with population and nightlight data to estimate the impact different natural hazard types had on local nightlight emissions across 5 different South East Asian countries.

The damage index is based on the USGS Shakemaps and the damage modeling is done using two data sets, the objective earthquake intensity data expressed by PGA and building inventory data. The latter data is the USGS

[2] Values below 2 constitute approximately 99.3 percent of the total. This was done due to the maximum VIIRS value being 154 and hence a density graph would be meaningless going from − 0.71 to 154. Also, any bin above 2 is very small and would not contribute to the graph.

[3] See next section for details on population layers.

building inventory for earthquake assessment, which provides estimates of the proportions (based on total number of buildings) of building types observed by country; see Jaiswal and Wald (2008). For Nepal the building type information was compiled from a World Housing Encyclopedia (WHE) survey. The WHE survey uses fraction of population who lives or works in buildings of different types as their definition of how the building mass is split up. The distribution of building types and mass are assumed to be homogenous within areas due to the lack of more granular spatial data. This is a strong assumption, but without detailed local data it is not possible to correct for. Preferably, one would want an extensive database with building by building damage, such as in Wang et al. (2016).

From the building and intensity data, we derive damage curves based on the curves constructed by the Global Earthquake Safety Initiative (GESI) project; see International and Regional Development (2001). GESI divide buildings into 9 different categories, which are then rated on different quality measures such as design, construction and materials used. Depending on the rating and whether the building is in a rural or urban area, one out of 16 damage curves (8 for urban and 8 for rural) are chosen as most likely to correlate to a building of the specific category and quality. In this article, it is assumed that all buildings in a category is of the same quality given that we have no further distributional or locational data.

More formally, to derive a cell i specific earthquake damage index, ED, the following equation is applied:

$$ED_{i,q,t} = DR_{i,k,t}^{pga_{k,q}} \quad q = 0, \ldots, 7$$

where DR is the damage ratio according to the peak ground acceleration, pga, and the urban–rural qualification k of cell i, defined for a set of 8 different building quality q categories.

The next step is to match the localized damage data with any intersecting VIIRS cell and assign the nightlight value to the corresponding month. For light cells that intersected several damage cells an average value was used. As earthquake damage estimates were modeled based on centroids, only the centroid intersection was used.

Finally, population data was aggregated up to the same cell size as the VIIRS data and then matched to summarize the total population in each nightlight cell. To include a cell in the data set, the aggregated population had to be a minimum of 5. This is based on the average household size in Nepal in 2010 being 5 (Libois and Somville 2018). Additionally, a cell was designated as either urban or rural depending on the number of people living in it. Our base case was 20, but numerous thresholds were explored, without it affecting the results significantly in either direction.

Following the construction of the data sets, two analytical methods were utilized to potentially identify and quantify the effect the earthquakes had on nightlight values. The first was a simple mean analysis. It consisted of two graphs; one with the mean of the nightlight values of cells that were struck by an earthquake and one with the cells that were not affected. Furthermore, it was broken down into two categories, one comparing light value means across all cells in Nepal and one comparing means only across cells in regions that were affected by the earthquakes.

The second set of analysis consists of fixed effects regressions with additional controls for time and spatial effects. To correct for potential heteroscedasticity, Driscoll-Kraay standard errors are used (Driscoll and Kraay 1998). The regression equation is as follows:

$$L_{i,t} = \beta_0 + \sum_{\mathrm{n}=0}^{12} \beta_{\mathrm{n}+1} ED_{i,q,t-n} + \theta_i + e_{i,t}$$

where $L_{i,t}$ is the light level in cell i in month t and $ED_{i,q,t}$ represents the damage curve value in the same cell and at the same time. Lags are allowed from month t to $\mathrm{t}-12$. β_0 is the intercept, θ_i are the cell fixed effects and $e_{i,t}$ is the error term.

The regressions are lagged for the 12 months following the hazards to allow for any short- and mid-term effects to materialize with the coefficients giving the effect that the earthquakes have on the nightlights for the month when the earthquake happens and the 12 subsequent months. The regression is run both nationally and at a province level.

A flow chart providing an overview of the methodology and data can be found in Fig. 4. Furthermore, an overview of the different data sources with resolutions and temporal and spatial scope can be found in Table 1. Finally, Fig. 5 provides a graphical comparison of the resolution of the different data sets.

Results

Figure 6 show the results from the mean analysis comparing the means of nightlight cells in the entire country (top panel) and the two most affected regions—Central and Western—in the bottom panel. The comparison is between cells that were damaged by the earthquake and cells that were not. In both cases, the nightlight values follow the same pattern implying that there is no difference between the two subgroups of cells.

Figure 7 shows the results for the second set of analysis, the fixed effect regressions for the entire country and for Central and Western. The coefficient values and

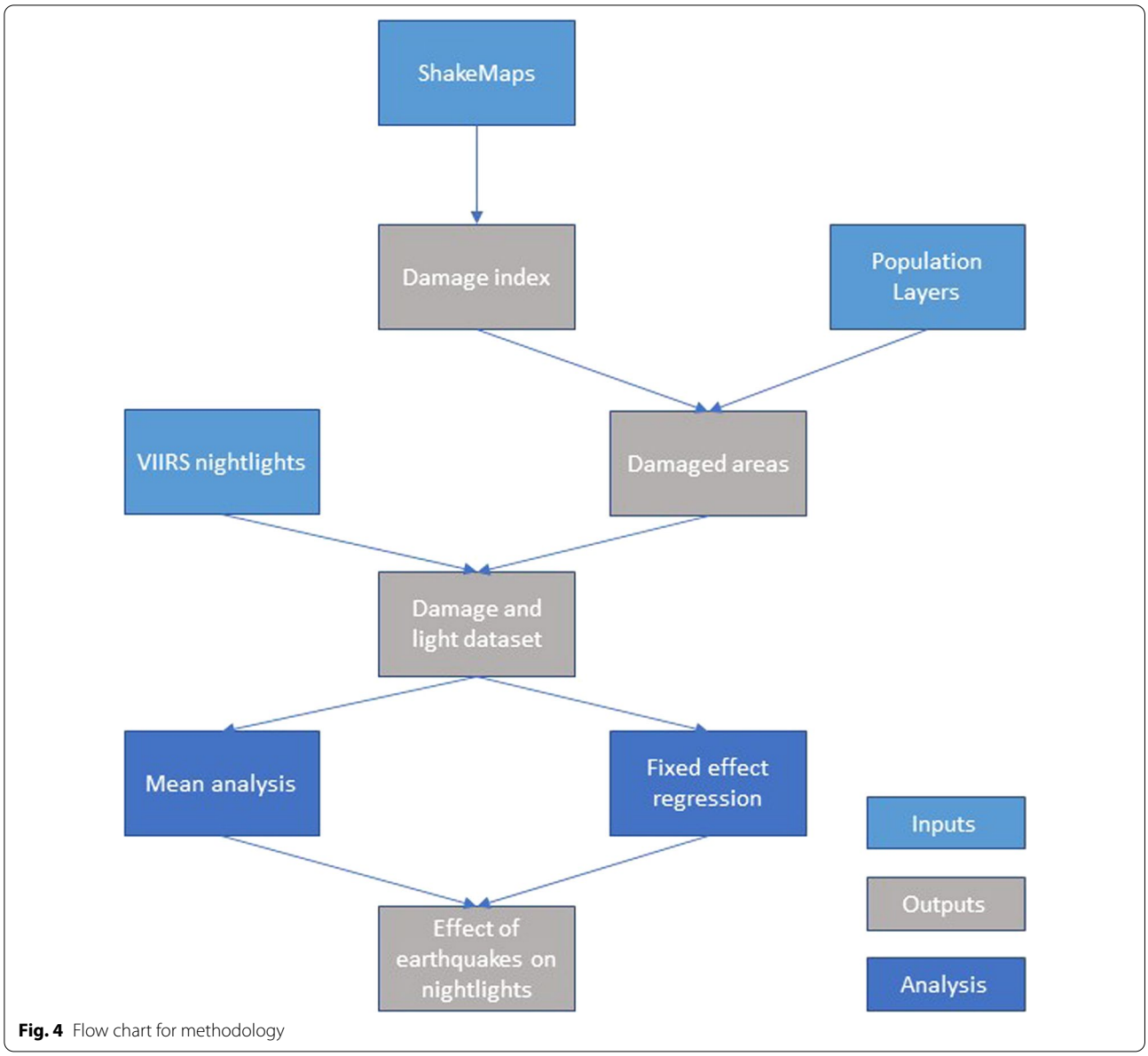

Fig. 4 Flow chart for methodology

Table 1 Overview of the different data sources

Data source	Type of data	Spatial resolution	Temporal res	Temporal coverage	Spatial coverage
VIIRS	Nightlights	15 arc-seconds	Monthly	2012-present	75 N 65S[a]
Worldpop	Population	3 or 30 arc-seconds	Annually or less	2000-present	Global
ShakeMaps	Earthquake	0.0167[ob]	One per EQ	1996-present[c]	Global

[a] Heavily dependent on time of year, i.e. during summer the hemispheres will have less nighttime coverage

[b] EMost are 0.0167°, but for Nepal it is 0.0333

[c] Earlier earthquakes are also covered, but the development did not start until 1996

significance are similar across both sets, with an initial negative shock during the month of the Gorkha earthquake followed by a positive effect for months 1 through 8. The positive effect is most pronounced for the first 4–6 months, before it tapers off. Months 6, 7, 10 and 11 are insignificant in the province analysis. In month 9, the country results show a negative and significant coefficient value, whereas Central and Western stay positive.

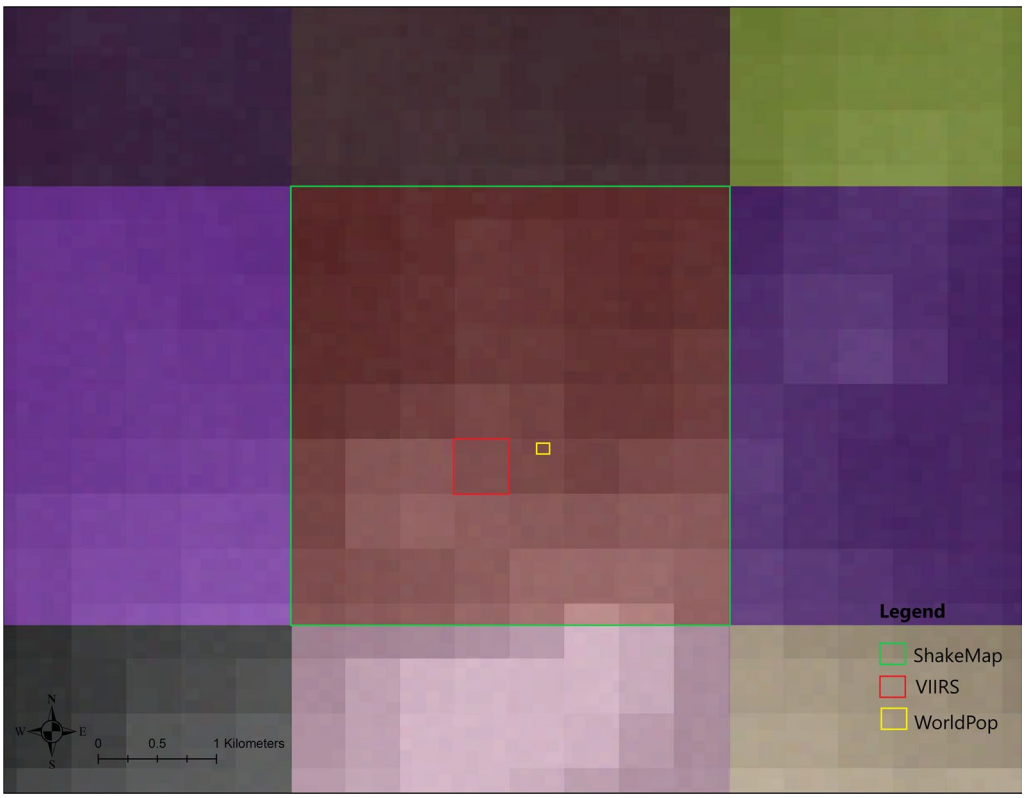

Fig. 5 Comparison of the spatial resolution of the ShakeMap, the VIIRS nightlight data and the WorldPop data

Afterwards, months 10 and 11 show a negative trend for both sets, while month 12 exhibits a strongly significant and positive jump.

Discussion

The aim of the paper was to get highly localized impact estimates by using VIIRS data combined with high-resolution population layers and spatially disaggregated damage data. The nightlight data has shown in prior studies, some of which use the Gorkha earthquake as their case study, that one can identify local effects from natural disasters (Zhao et al. 2018; Gao et al. 2020). A key assumption is that damage can be linked to economic output. This is not necessarily true for cases where the damages are structural or human in nature. However, it is assumed that our modelled structural damages will affect the nightlight values, which has shown a close link with economic output, see for example Henderson et al. (2012) or Michalopoulos and Papaioannou (2014).

Our analysis rests on several assumptions, which can differ based on the area and time span being analyzed. Firstly, the population data is used to define which areas are populated and whether any populated area is considered to be rural or urban.[4] The former threshold was set at 5, which is in line with an average household size in Nepal. Whereas for the latter numerous thresholds were explored, ranging from 5 (all urban) to 100. However, the choice had little impact on the regression or mean results. When running the regressions for urban areas only, i.e. only for cells that were deemed to be urban, the coefficient values change, but the significance and direction of the signs are the same as for the primary analysis. In addition, we visually inspected the data to check for any differences depending on which year of population was chosen. We found no discernible difference in terms of populated areas and when comparing the population per pixel between years, the differences were very small and indicative of a simple application of growth trend that has been interpolated across the cells.

Secondly, when modeling the damage, the building quality assumption will have an impact on the sustained

[4] We also considered which data set to use as our population basis. We did use 2015, and when comparing the data with 2011, the differences are very small and implies that a simple growth trend has been used to adjust the population numbers.

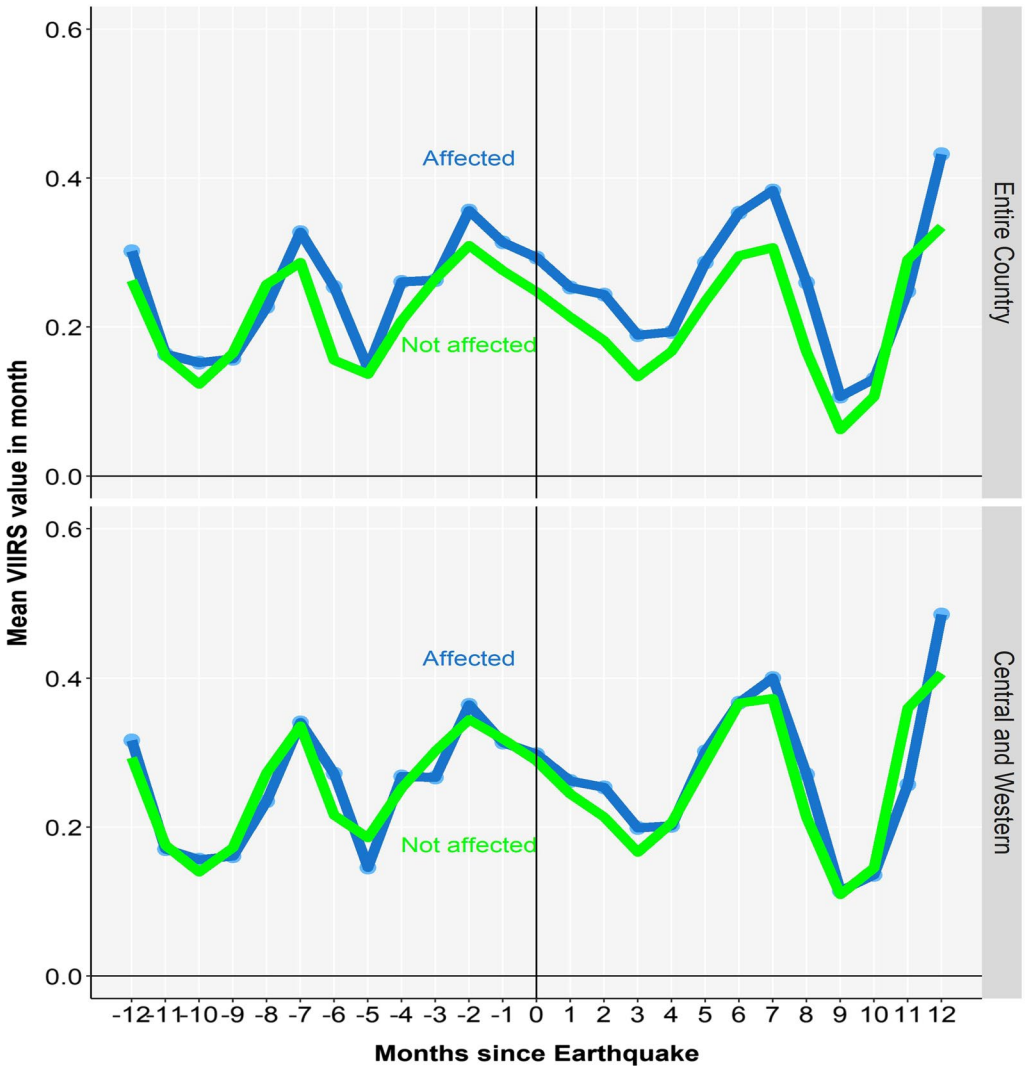

Fig. 6 Mean of nightlight cell values for Nepal and the Central and Western districts split between cells that were affected by earthquakes and those that were not

damage as well as the final impact estimates on nightlights. When the analysis was performed, we did find a non-negligible effect on the estimates but lacking any meaningful information a mean quality assumption of 4 was used.

Related to the first two points, assuming that the building types and quality are homogenously distributed across Nepal is not likely to be true given the diverse topography and climate of Nepal. However, lacking more detailed data on the distribution it is neigh on impossible to correct for. The rural/urban distinction might help alleviate some of the issues and given how the results did not change with differing thresholds it gives some confidence in the results.

Fourthly, the nightlight values depend on two assumptions. The first one regards missing nightlight values, usually missing due to lack of cloud free observations. When no value was present, it was linearly interpolated from the last light value before the missing observation and the first light value after the observation. Another option that was explored, was to use the prior year's value, but this did not affect the final estimates. The second assumption was related to the treatment of VIIRS values close to or below 0. When the VIIRS images are processed a dark offset is deducted from the raw day/night value. This offset is sometimes severely impacted by airglow leading to negative light

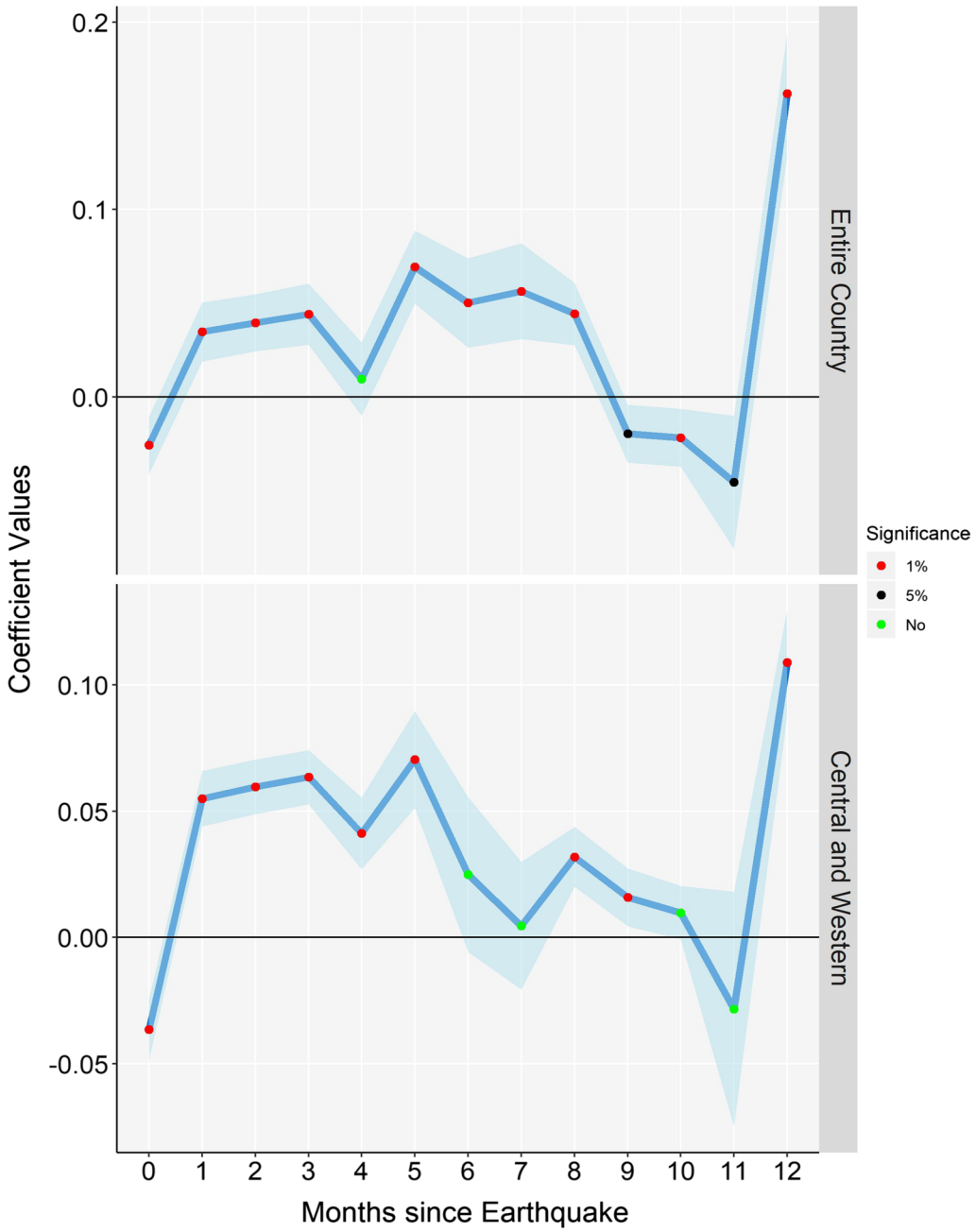

Fig. 7 Regression results for Nepal and the Central and Western districts

values. To account for this in our analysis, several options were explored. Firstly, the regressions were run with any light value below 0.1 set to 0. Then absolute values were used with any absolute value below thresholds of 0.1, 0.3 and 0.5 set to 0. Overall, the threshold choice only had a minor quantitative impact on the coefficients. Recently, the papers from Gao et al. (2020) and Zhao et al. (2020) show that one can—and probably should—detrend and clean the data to get more consistent and less volatile nightlight values.

Finally, the nightlight data shows that during monsoon season, the number of cloud free days is on average very low. This is partially corrected for by interpolating the nightlight values for the month before and after a month with no cloud free days and also tested for by using the previous year's nightlight value. This is not optimal and

could impact the estimates depending on how the lack of observations is distributed, but we are unaware of any other or better way to correct for the lack of observations.

As for the results, the mean comparisons of the nightlight values in Fig. 5 yielded no difference between affected cells and cells that were not damaged by the earthquake. As can be seen, the trends are the same for both sets of cells and there are several peaks and throughs throughout the period, some of which may be seasonal. The nightlight values exhibit a low during the winter months and a high in fall and late fall. Some of this effect could be due to measurement differences and cloud cover, but it might also be caused by differences in use of energy and covering up lights during the winter months. The lack of difference between the two means could be due to aid and relief efforts targeting all areas but given the inherent volatility and noise in the VIIRS values it is more likely that any quantitative effects on the local economy has not been strong enough to be captured by the VIIRS data when performing such a simple analysis. To further test this we performed a pre-post analysis where we compared the change in nightlight value for the month before the earthquake (March) with the value for May and June. In this instance, the cells affected by the earthquake experienced a slightly smaller drop in absolute values (-0.049 vs -0.057). However, due to the higher mean absolute value of the affected cells, the percentage change was -16% versus -22%. When performing a t-test between the two sample means, we find the difference to be significant at a 5% level, indicating that the affected cells experienced a smaller drop than the non-affected ones. One possible explanation for this could be the influx of aid or an inherent difference between the two groups. To explore this further, we performed a mean comparison between the nightlight values for both affected and non-affected cells for May and June in 2012–2014 versus the mean in 2015. Once again, we find that the growth for the affected cells is bigger, i.e. the nightlight value for affected cells is relatively higher than for the non-affected cells. This could indicate that the two groups of cells are on different trajectories, that potentially the affected cells are in more urban areas. This could also explain why the fixed effects regressions identify a significant difference.

The regression results did find that a statistical and significant effect occurred in cells that were damaged by the earthquakes. One potential explanation for the nightlight value impact could be that in the month of the quake, there is a nightlight loss due to the damages. Then, in the following months, there is an increased activity from aid, repairs and rebuilding. Finally, one sees a decline followed by a negative effect that could signify the end of the rebuilding efforts and the aid influx. However, the sudden and significant coefficient increase in month 12 differs from the expected pattern, which is a return to non-significance and coefficient values close to 0, i.e. the earthquake should not impact nightlight values for a very long period of time. When exploring the underlying data and general information about Nepal, we found no spatial or seasonal pattern in the data or information about new power plants or other events that could have caused the spike, leading us to believe that it might be due to the general volatility of the data. Increasing the lag period is also problematic as it will decrease the sample size and is likely to capture other events that can potentially bias the results. Once the VIIRS data is available for longer periods both pre and post events it will be more feasible to do longer lags and potentially identify more long-term effects, although it can always be argued that any long-term impact—in particular when one does month by month analysis—are unlikely to be correctly quantified due to the many factors that impact light and the measurements. However, this can be an interesting avenue for future research.

Finally, Fig. 8 depicts a comparison between our modelled damage, gridded out via a kriging algorithm, and the Copernicus Emergency Management Service (EMS) grading map for Kathmandu. The Copernicus map uses satellite images from DigitalGlobe and Pleiades CNES at 0.5 m resolution to visually compare ex-post and ex-ante images and identify changes and potential damages. The focus in the Copernicus maps is at a building level, while our modelling focuses on a much more aggregate level making the two data sets difficult to compare. In addition, the Copernicus maps are only produced for 8 areas that cover approximately 35 square kilometres each. With this in mind, Fig. 7 is provided as a visual comparison of how our model performed versus the Copernicus map. Looking at the main area of damage as identified in the Copernicus map, we find that the outlined rectangular cell with the most damaged buildings map is seemingly more damaged than the neighbouring cells. However, looking at the overall map, the marked cell does not stand out. This is most likely due to a combination of much lower resolution data as well as the kriging algorithm, which leads to a smoothing of the damages.

Conclusion

Having used the VIIRS data as an economic proxy one finds that the earthquakes in Nepal in 2015 did impact the local economic activity if one uses fixed effects regressions. Overall, there is an initial decrease when the shock occurs, followed by an increase in activity once aid and relief efforts have started. This is consistent with what one would expect, however, with the

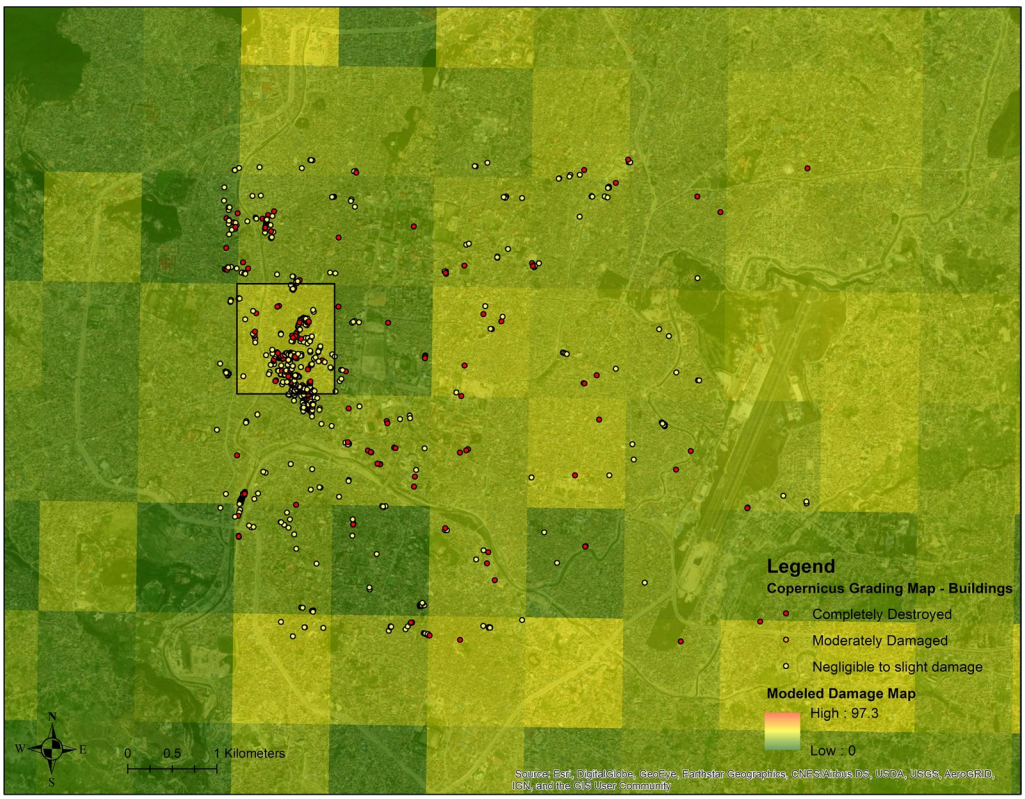

Fig. 8 Comparison for Kathmandu between Copernicus grading map and modelled damage map

amount of noise and cloud cover in the underlying VIIRS data some caution is in order.

Potential future research within the area could focus on other large-scale earthquakes or natural hazard types as the methodology is easily scaled and depends on few inputs. Another option is to explore other algorithms or secondary data to potentially achieve more consistent and comparable nightlight measurements.

Acknowledgements
This paper was funded by the global knowledge program of the World Bank's Poverty and Equity Global Practice.

Authors' contributions
TT: analysis, data gathering, idea, writing, editing. ES: editing, writing, idea, funding. ES: editing, writing, idea. All authors read and approved the final manuscript.

Availability of data materials
The data used in this study were derived from the following resources available in the public domain: These data were derived from the following resources available in the public domain: *Population data* Worldpop: https://www.worldpop.org/project/categories?id=3. *Nightlights data* VIIRS: https://eogdata.mines.edu/download_dnb_composites.html. *Earthquake data* USGS Shakemaps: https://earthquake.usgs.gov/earthquakes/search/. Building inventory data: https://pubs.er.usgs.gov/publication/ofr20081160.

Declarations

Competing interests
The authors declare no competing interests.

Author details
[1]Department of Economics, University of Bern, Schanzeneckstrasse 1, 3001 Bern, Switzerland. [2]The World Bank Group, Poverty and Equity Global Practice, Washington, DC, USA.

Received: 9 September 2021 Accepted: 26 December 2021
Published online: 03 January 2022

References

Agency, Federal Emergency Management (2006) HAZUS-MH MR2 Technical Manual. Washington, DC

Baragwanath K, Goldblatt R, Hanson G, Khandelwal AK (2019) Detecting urban markets with satellite imagery: an application to India. J Urban Econ. https://doi.org/10.1016/j.jue.2019.05.004

Chen Xi, Nordhaus W (2015) A test of the new VIIRS lights data set: population and economic output in Africa. Remote Sens 7:4937–4947. https://doi.org/10.3390/rs70404937

Chen Xi, Nordhaus WD (2019) VIIRS nighttime lights in the estimation of cross-sectional and time-series GDP. Remote Sens. https://doi.org/10.3390/rs11091057

Corbane C, Kemper T, Freire S, Louvrier C, Pesaresi M (2016) Monitoring the Syrian humanitarian crisis with the JRC's global human settlement layer and night-time satellite data. Publications Office of the European Union, Luxembourg, pp 1–14
De Groeve T, Annunziato A, Gadenz S, Vernaccini L, Erberik A, Yilmaz T (2008) Real-time impact estimation of large earthquakes using USGS Shakemaps. In: Proceedings of IDRC2008, Davos, Switzerland
Driscoll J, Kraay A (1998) Consistent covariance matrix estimation with spatially dependent panel data. Rev Econ Stat 80:549–560
Elliott RJR, Strobl E, Sun P (2015) The local impact of typhoons on economic activity in China: a view from outer space. J Urban Econ 88:50–66. https://doi.org/10.1016/j.jue.2015.05.001
Gao S, Chen Y, Liang L, Gong A (2020) Post-earthquake night-time light piecewise (PNLP) pattern based on NPP/VIIRS night-time light data: a case study of the 2015 Nepal earthquake. Remote Sens 12:2009. https://doi.org/10.3390/rs12122009
Gibson J, Olivia S, Boe-Gibson G (2019) A test of DMPS and VIIRS night lights data for estimating GDP and spatial inequality for rural and urban areas. Working papers in economics, University of Waikato. https://ideas.repec.org/p/wai/econwp/19-11.html
Gillespie TW, Frankenberg E, Chum KF, Thomas D (2014) Night-time lights time series of tsunami damage, recovery, and economic metrics in Sumatra, Indonesia. Remote Sens Lett 5:286–294. https://doi.org/10.1080/2150704X.2014.900205
Henderson JV, Storeygard A, Weil DN (2012) Measuring economic growth from outer space. Am Econ Rev 102:994–1028. https://doi.org/10.1257/aer.102.2.994
Hodler R, Raschky PA (2014) Regional favoritism. Q J Econ 129:995–1033. https://doi.org/10.1093/qje/qju004
INFORM (2019) 07. http://www.inform-index.org/Portals/0/Inform/2019/country_profiles/NPL.pdf. Accessed July 2019
International, GeoHazards, and United Nations Centre Regional Development (2001) Final report: global earthquake safety initiative (GESI) pilot project. Report, GHI, 86 p
Jaiswal KS, Wald DJ (2008) Creating a global building inventory for earthquake loss assessment and risk management: US Geological Survey Open-File Report 2008-1160. Technical report, USGS, 103 p
Jean N, Burke M, Xie M, Davis WM, Lobell DB, Ermon S (2016) Combining satellite imagery and machine learning to predict poverty. Science 353:790–794. https://doi.org/10.1126/science.aaf7894
Klomp J (2016) Economic development and natural disasters: a satellite data analysis. Glob Environ Chang 36:67–88. https://doi.org/10.1016/j.gloenvcha.2015.11.001
Libois F, Somville V (2018) Fertility, household size and poverty in Nepal. World Dev 103:311–322. https://doi.org/10.1016/j.worlddev.2017.11.005
Michalopoulos S, Papaioannou E (2014) National institutions and subnational development in Africa. Q J Econ 129:151–213. https://doi.org/10.1093/qje/qjt029
Nguyen CN, Noy I (2019) Measuring the impact of insurance on urban earthquake recovery using nightlights. J Econ Geogr 20:857–877. https://doi.org/10.1093/jeg/lbz033
Sahoo S, Gupta PK, Srivastav SK (2020) Inter-calibration of DMSP-OLS and SNPP-VIIRS-DNB annual nighttime light composites using machine learning. Gisci Remote Sens 57:1144–1165. https://doi.org/10.1080/15481603.2020.1848323
Skoufias E, Strobl E, Tveit T (2021) Can we rely on VIIRS nightlights to estimate the short-term impacts of natural hazards? Evidence from five South East Asian countries. Geomat Nat Haz Risk 12:381–404. https://doi.org/10.1080/19475705.2021.1879943
Skoufias E, Strobl E, Tveit T (2017) Natural disaster damage indices based on remotely sensed data: an application to Indonesia (English). World Bank policy research working paper no. 8188
Uprety S, Cao C, Gu Y, Shao X, Blonski S, Zhang B (2019) Calibration improvements in S-NPP VIIRS DNB sensor data record using version 2 reprocessing. IEEE Trans Geosci Remote Sens 57:9602–9611. https://doi.org/10.1109/TGRS.2019.2927942
Wang F, Miyajima M, Dahal R, Timilsina M, Li T, Fujiu M, Kuwada Y, Zhao Q (2016) Effects of topographic and geological features on building damage caused by 2015.4.25 Mw7.8 Gorkha earthquake in Nepal: a preliminary investigation report. Geoenviron Disasters 3:7. https://doi.org/10.1186/s40677-016-0040-2
Worldpop (2017) Nepal 100m population, version 2. University of Southampton. https://doi.org/10.5258/SOTON/WP00531
Xu C, Tian Y, Zhou B, Ran H, Lyu G (2017) Landslide damage along Araniko highway and Pasang Lhamu highway and regional assessment of landslide hazard related to the Gorkha, Nepal earthquake of 25 April 2015. Geoenviron Disasters 4:14. https://doi.org/10.1186/s40677-017-0078-9
Zhao N, Hsu F-C, Cao G, Samson EL (2017) Improving accuracy of economic estimations with VIIRS DNB image products. Int J Remote Sens 38:5899–5918. https://doi.org/10.1080/01431161.2017.1331060
Zhao X, Bailang Yu, Liu Y, Yao S, Lian T, Chen L, Yang C, Chen Z, Jianping Wu (2018) NPP-VIIRS DNB daily data in natural disaster assessment: evidence from selected case studies. Remote Sens 10:1526. https://doi.org/10.3390/rs10101526
Zhao N, Liu Y, Hsu F-C, Samson EL, Letu H, Liang D, Cao G (2020) Time series analysis of VIIRS-DNB nighttime lights imagery for change detection in urban areas: a case study of devastation in Puerto Rico from hurricanes Irma and Maria. Appl Geogr 120:102222. https://doi.org/10.1016/j.apgeog.2020.102222

Publisher's Note